Journal of Nuclear Materials 393 (2009) 425–432

Contents lists available at ScienceDirect

Journal of Nuclear Materials

journal homepage: www.elsevier.com/locate/jnucmat

Tensile–shear correlations obtained from shear punch test technique using a modified experimental approach

V. Karthik *, P. Visweswaran, A. Vijayraghavan, K.V. Kasiviswanathan, Baldev Raj

Metallurgy and Materials Group, Indira Gandhi Centre for Atomic Research, Kalpakkam 603102, India

ARTICLE INFO

Article history:
Received 11 February 2009
Accepted 23 June 2009

ABSTRACT

Shear punch testing has been a very useful technique for evaluating mechanical properties of irradiated alloys using a very small volume of material. The load–displacement data is influenced by the compliance of the fixture components. This paper describes a modified experimental approach where the compliances of the punch and die components are eliminated. The analysis of the load–displacement data using the modified setup for various alloys like low carbon steel, SS316, modified 9Cr–1Mo, 2.25Cr–1Mo indicate that the shear yield strength evaluated at 0.2% offset of normalized displacement relates to the tensile YS as per the Von Mises yield relation ($\sigma_{ys} = 1.73\tau_{ys}$). A universal correlation of type UTS = $m\tau_{max}$ where m is a function of strain hardening exponent, is seen to be obeyed for all the materials in this study. The use of analytical models developed for blanking process are explored for evaluating strain hardening exponent from the load–displacement data. This study is directed towards rationalizing the tensile–shear empirical correlations for a more reliable prediction of tensile properties from shear punch tests.

1. Introduction

The shear punch test is a very useful mechanical test technique for evaluating the mechanical properties viz. yield strength, maximum strength and strain hardening exponent using very small volumes of material [1]. The driving force for development of this technique has been the material development programmes for fusion and fission reactors. The small volumes of specimens could be easily fitted into the existing irradiation space and permitted easy handling due to low radioactivity for mechanical property evaluation [2]. As a spin-off, it has a variety of other applications in situations where conventional mechanical tests are not possible such as weld joints [3], coatings and failure analysis.

The shear punch (ShP) test technique involves slow blanking of a thin disc material clamped between a set of dies at a constant speed as shown schematically in Fig. 1. The deformation occurs in the small annular region of the punch–die clearance. The load–displacement curve (LDC) obtained during the blanking operation (Fig. 2) is very similar to that obtained in a conventional uniaxial tensile test and the properties obtained by analyzing the ShP test curve can be correlated to the corresponding conventional tensile properties.

Many investigators have evolved the experimental test setup and the method of analyzing the LDC over a period of time. In the initial period of its development, investigators used the crosshead movement as an approximate measure of punch displacement. Finite element simulation and analysis of the shear punch test by Toloczko et al. [4] revealed that the compliance in the test frame and fixturing had a profound effect on the shape of the LDC. To minimize the effects of test frame compliance on the LDC, the test setup was modified suitably to accommodate a displacement sensor across the test fixture [5] or coupled to the moving punch [6,7].

The other aspect that has caught the attention of many investigators is the accurate measurement of the yield load from the LDC. The point of deviation from linearity of the initial portion of LDC was first used as an approximate measure of the shear yield load [2]. However, for materials exhibiting a very smooth transition from the linear to the non-linear deformation, this method of locating the yield load resulted in considerable scatter. In one of our earlier studies, it was shown that online acoustic emission monitoring during the test led to accurate prediction of the yield load [8]. Researchers subsequently adopted the method of measuring yield stress at an offset shear strain analogous to the offset procedure used in tensile testing.

To rationalize the methodology for shear yield strength determination, Guduru et al. [9] carried out finite element analysis (FEA) of the initial stages of punch displacement. Based on the development of plastic deformation zone completely through the specimen thickness, they concluded that an offset of 0.15% of initial linear portion of FEA generated stress–normalized displacement curve represent the shear yield stress. However, this corresponded to an offset of 1% in the actual experiments due to the compliance effects of the test fixtures. The shear yield strength corresponding to 1% offset in their study satisfied the relation $\sigma_{ys} = 1.77\tau_{ys}$ which

* Corresponding author. Tel.: +91 44 27480122; fax: +91 44 27480356.
E-mail address: karthik@igcar.gov.in (V. Karthik).

0022-3115/$ - see front matter © 2009 Elsevier B.V. All rights reserved.
doi:10.1016/j.jnucmat.2009.06.027

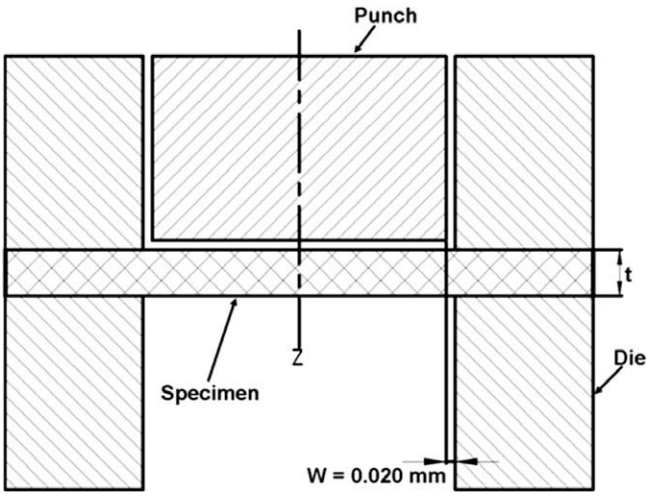

Fig. 1. Schematic of the shear punch test technique.

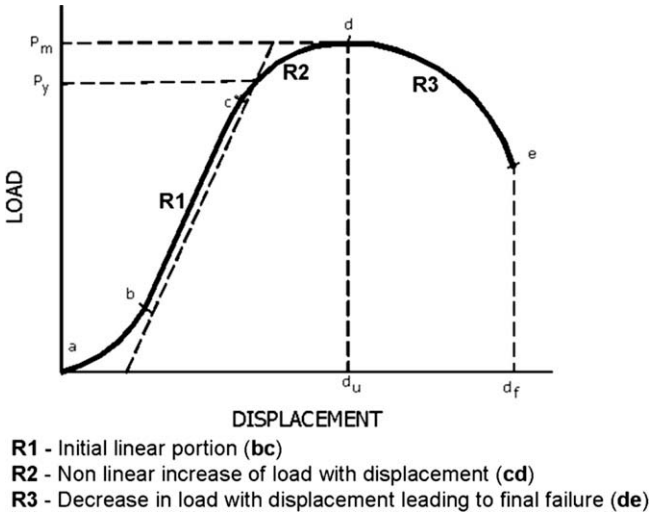

Fig. 2. Typical load–displacement plot obtained in a shear punch test.

is in close agreement with the Von Mises yield relation. Studies by Toloczko et al. [6] using a modified test setup also indicated that the yield strength determined using the "1% offset" shear strain correlated well with tensile yield strength as per the Von Mises yield relation. It may be noted that both Toloczko et al. and Guduru et al. have measured the punch displacement by a displacement sensor coupled to the moving punch. The linear correlation between the ultimate tensile strength (UTS) and shear maximum strength has been generally found to obey the linear relation of type UTS = $A\tau_{max} + B$ with a range of values for A and B for various alloy classes [10].

In the present work, a modified shear punch experimental setup has been used with an aim to eliminate the compliance effects of punch and die components on the test data. In the modified test setup, the displacement is measured using a sensor attached to the bottom of the specimen. With this arrangement, the compliance effect of the punch on the measured displacement is eliminated. The LDC obtained from the modified setup is also corrected for the compliances arising out of the dies and associated fixturing through elastic loading tests with thick specimens. The corrected LDC is analyzed for various materials like carbon steel, chrome-moly steels, austenitic stainless steel, copper and aluminum alloys. The shear yield strengths evaluated at offsets of 0.2%, 0.5% and 1% are compared with the tensile YS for the various materials. The offset criterion which produces the best fit between tensile YS and shear yield strength is established and compared with published results. The nature of correlations obtained for maximum strength in ShP test and the corresponding UTS is also investigated. It is found that UTS can be related to shear maximum strength through a function involving the strain hardening exponent without any alloy specific constants. Finally an attempt is made to evaluate the strain hardening exponent from load–displacement data using analytical models developed for blanking process.

2. Experimental procedure

2.1. Shear punch test setup

Fig. 3 shows the schematic of the shear punch test fixture developed at the authors' laboratory. The test fixture consists of a flat punch of 3 mm diameter made of a hardened tool steel (RC 62) and a set of dies between which the specimen is clamped. The diameter of the receiving hole in the lower die is 3.04 mm. The test fixture is placed on the compression platens of a universal test machine for carrying out the test. The load during the punch operation is measured using a standard load cell of 4 kN. A linear variable differential transformer (LVDT) of range ±2.5 mm is fixed at the bottom of the test fixture as shown in Fig. 4. The LVDT is coupled to the center of the specimen bottom using a stiff tungsten carbide rod to measure the specimen displacement. The test fixture, LVDT and the connecting rod are placed in line for accurate measurement of the specimen deformation. The experimental setup has also provisions for positioning the LVDT at the top of the moving punch as shown in Fig. 5. This was to enable the comparison of the LDC's obtained using the two methods of displacement measurement. The load and displacement data are acquired through a 16 bit resolution data acquisition system built in the test machine controller.

2.2. Materials

Six different materials namely low carbon steel, AISI SS316, 2.25Cr–1Mo steel, modified (Mod) 9Cr–1Mo steel, aluminum and copper were chosen for the present study. The chemical composi-

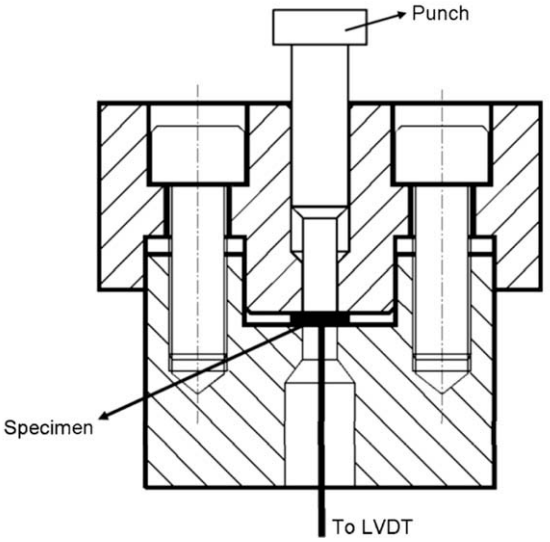

Fig. 3. Schematic of the shear punch test fixture.

Fig. 4. The experimental setup of shear punch tests showing the LVDT attachment coupled to the bottom of the specimen clamped in the test fixture.

Fig. 5. The experimental setup where LVDT is coupled to moving punch for measuring the displacements.

tion of the various steels and their thermo-mechanical conditions are given in Table 1.

2.3. Tensile tests

Conventional flat tensile test specimens (25 mm gage length) were machined from the various materials and tensile tests were carried out at a nominal strain rate of 3×10^{-4} s^{-1} at ambient temperature (298 K) using a computer controlled universal testing machine as per ASTM E 8. Two tests were performed for each material and the average value is reported.

2.4. Shear punch test

Small disc specimens of 8 mm diameter and 1.0 mm thickness were EDM (electric discharge machining) wire cut from the various materials and their surfaces were gently ground using SiC 600 grit to a final thickness in the range of 0.3–0.8 mm (±0.005 mm). Shear punch tests were performed using a universal test machine at room temperature and at a constant crosshead speed of 1.6×10^{-3} mm/s. Tests were conducted on specimens of different thicknesses to study the thickness effect on the LDC. Four samples were tested for each thickness of the material and the average values are reported.

To determine the compliance of the test fixture and the components of LVDT fixturing, a sufficiently thick specimen (3 mm thickness) of high speed steel was elastically deformed to nominal peak loads achieved in actual shear punch tests. The load–deflection data obtained was used to compute the compliance of the test setup.

3. Results and discussion

3.1. Shear punch test curves and compliance correction

A typical load–displacement curve for AISI 316 obtained using the modified test setup is shown in Fig. 6. The LDC obtained using the LVDT positioned at the top of the moving punch is superimposed for comparison. The initial non-linearity and the effect of the punch compliance can be observed in the latter curve. In the modified setup, the initial loading of the punch on the specimen instantaneously produces measurable displacement at its bottom surface. This clearly reflects that the displacement measured closely represents the punch tip displacement. Thus the compliance of the punch and the fixturing above the specimen plane are completely eliminated by this modified experimental setup.

The compliance of the fixture components below the specimen plane like bottom die and the LVDT setup are deduced by analyzing the load–displacement plots of elastic loading tests performed on thick specimens. The compliance (C) which is the inverse of slope of the LDC (Fig. 7) is estimated to be about 1.9×10^{-5} mm/N. The actual displacement d_c in the shear punch tests are corrected as

$$d_c = d - (P \times C), \tag{1}$$

where d is the displacement measured by LVDT and P is applied load. Fig. 8 shows the two curves before and after correcting for the compliance effects, respectively. The change in the slope of the initial loading line as a result of the compliance correction can be well observed.

3.2. Effect of specimen thickness

Tests with specimens of different thicknesses ranging from 0.3 to 0.8 mm indicated a systematic shift in the LDC. The load–dis-

Table 1
Chemical composition of the various steels used in this study.

In wt.%	C	Si	Mn	Cr	Mo	Ni	N	Nb	V	Fe	Condition
AISI type 1025 carbon steel	0.23		0.40							Bal	Annealed
2.25Cr–1Mo steel	0.06	0.18	0.48	2.18	0.93					Bal	Normalized and tempered
Mod 9Cr–1Mo steel	0.096	0.32	0.46	8.72	0.90	0.10	0.05	0.08	0.22	Bal	Normalized and tempered
AISI 316 SS	0.06	1.0	2.0	17.0	2.4	12.0	–	–	–	Bal	Annealed

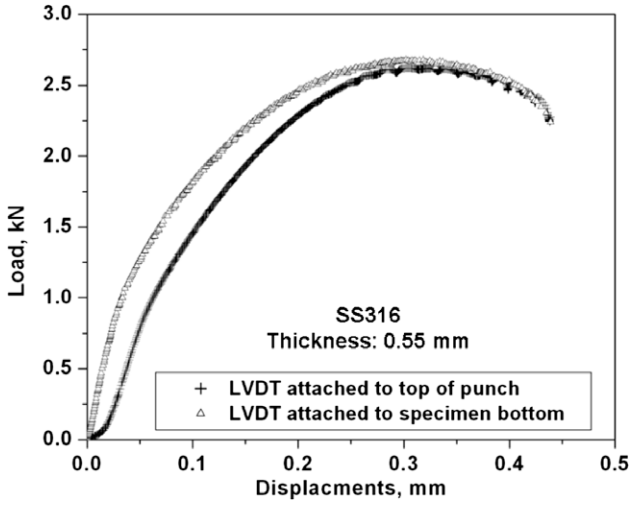

Fig. 6. Shear punch test load–displacement curve obtained for SS316 with the modified setup superimposed on that obtained using LVDT attached to punch top.

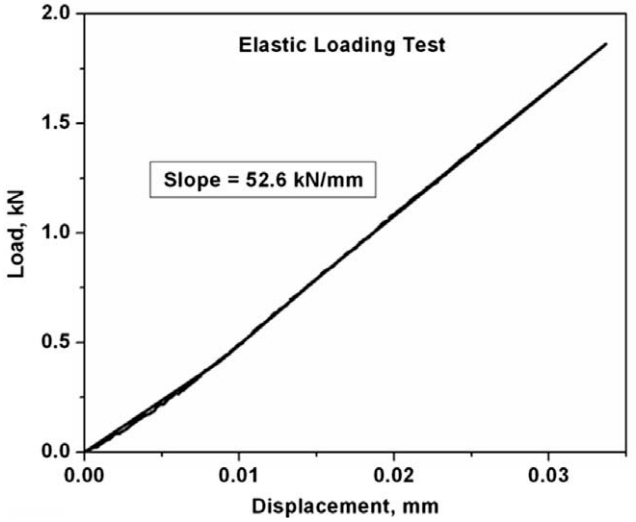

Fig. 7. Load–displacement plots of elastic loading tests carried out to compute the compliances of the experimental setup.

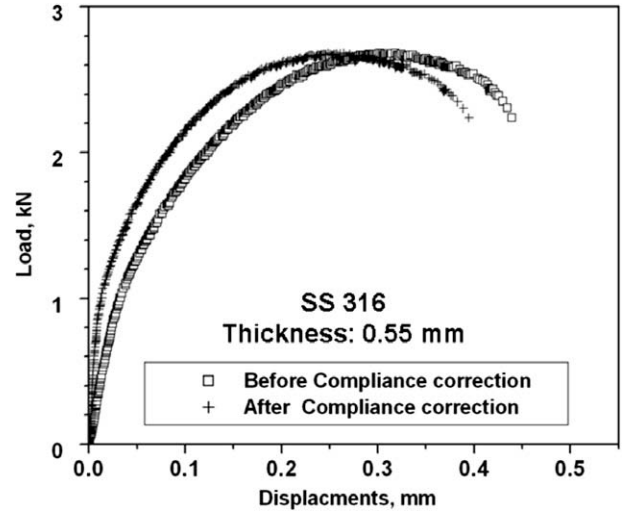

Fig. 8. Comparison of the load–displacement plots obtained for SS316 using the modified experimental setup before and after applying the compliance correction.

placement data is converted to stress–normalized displacement data using the following expressions:

$$\text{Shear stress} \quad \tau = \frac{P}{2\pi r t}, \tag{2}$$

$$\text{Normalized displacement} \quad \delta = \frac{d_c}{t}, \tag{3}$$

where P is the applied load, t is the specimen thickness, r is the average of punch and lower die radius and d_c is the displacement corrected for compliance effects. When the LDC for SS316 of varying thickness samples are scaled to shear stress–normalized displacement curves as shown in Fig. 9, the normalized curves overlapped well except for thickness less than 0.5 mm. Though the shear maximum strength is the same for all thicknesses, there is a change in slope of the initial loading line for specimen thickness less than 0.5 mm. Similar deviations of the normalized curves for lower thickness specimens were noticed for all the materials studied. This change in the initial slope of the normalized curves for lower thickness is likely due to the loading caused by bending or compression of thin specimens [7]. Based on these observations, the normalized curves for thickness above 0.5 mm which overlapped irrespective of the specimen thickness were only analyzed.

3.3. Tensile–shear strength correlations

The stress–normalized displacement curves for the various materials studied are plotted in Fig. 10. The shear maximum strength is computed from the peak points of the plots. The value of shear stress at a specified offset from linearity is used to define the shear yield strength. Using this operational definition, the shear YS was computed at offsets of 0.2%, 0.5% and 1% of the normalized displacement. The standard deviations for the measured shear maximum and yield strengths were ±3% and ±6% of the respective average values. These values are given in Table 2 along with the corresponding tensile properties for the various materials studied.

3.3.1. Yield correlation

The plot of the tensile YS with shear YS determined for the various offsets and the corresponding fit parameters namely the slope, regression coefficient and the standard deviation of the fit are given in Fig. 11. It can be seen that out of the three offset definitions for the shear YS, the 0.2% offset produces the best fit with a regression coefficient of $R^2 = 0.99$ and a standard deviation of ±17 MPa.

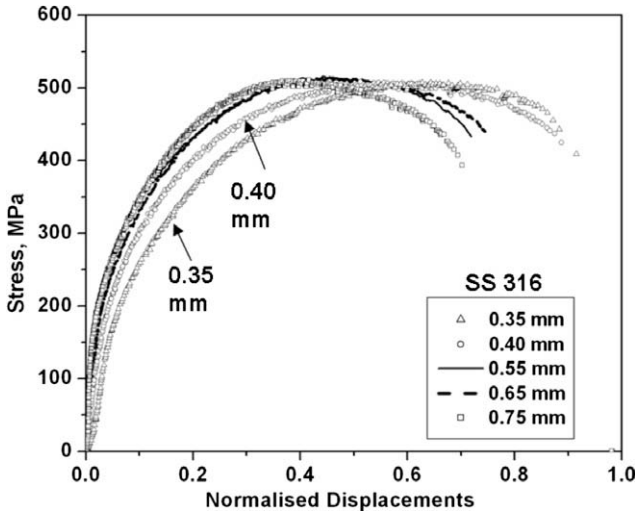

Fig. 9. ShP test curves of SS 316 samples with different thicknesses.

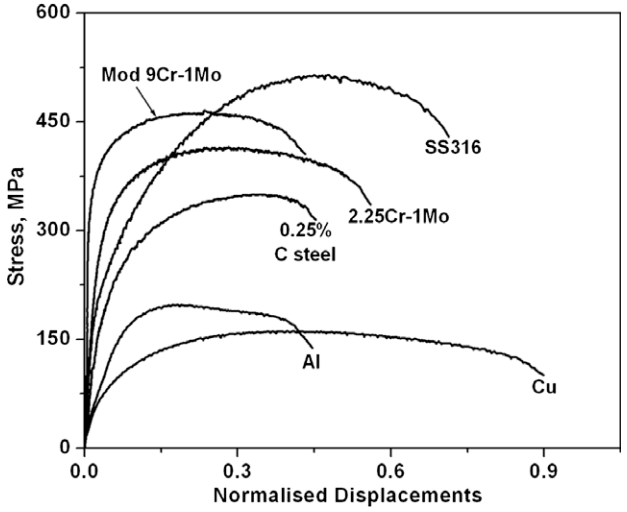

Fig. 10. The stress–normalized displacement curves for various materials.

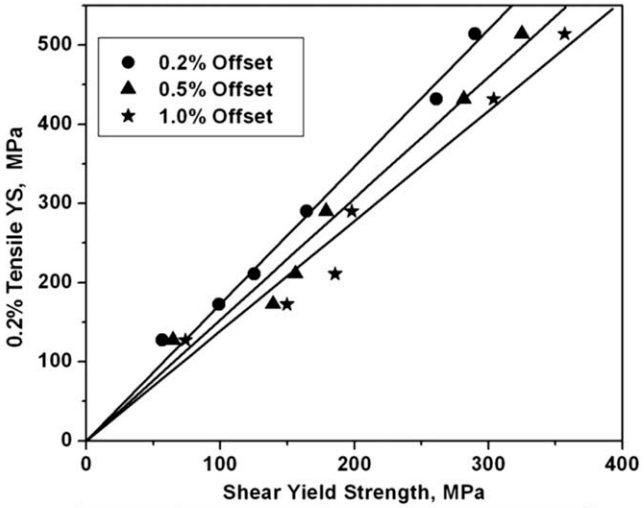

Offset	Slope of fit	Regression Coefficient R^2	Standard Deviation SD, MPa
0.2%	1.73 ± 0.037	0.990	17.185
0.5%	1.53 ± 0.053	0.968	27.34
1.0 %	1.38 ± 0.054	0.961	30.63

Fig. 11. Linear fit between the tensile and shear yield strengths of various materials for different offsets.

The offset definition of 0.2% is much less than the value of 1% reported by Toloczko and Guduru. A larger percentage offset required in their experiments was due to the finite compliances of the die and punch components. In the present investigation, these compliances are eliminated through (i) the use of LVDT at bottom of the specimen and (ii) corrections through elastic loading tests. This resulted in steeper loading curve enabling accurate evaluation of shear YS at 0.2% offset. This offset is in close agreement with the FEA offset of 0.15% obtained by Guduru et al. [9] with rigid punch, die and holder components. The equation of linear fit obtained between tensile YS and 0.2% offset shear yield strength is $\sigma_{ys} = 1.73\tau_{ys}$ which is exactly the same as Von Mises yield relation for shear deformation.

The nature of tensile–shear correlations obtained from shear punch tests has been a subject of debate over a period of years. Early studies led to development of material specific correlations of type $\sigma = A\tau + B$ for yield and maximum strength with a range of A and B values for various alloy class. With the insights provided by FEA and improvements in displacement measurement for compliance corrections, the yield correlation simplified into a universal equation of type $\sigma_{ys} = A\tau_{ys}$ with a material independent value for A. This work establishes that the offset definition for shear yield strength with the modified experimental setup is 0.2% and the shear YS so computed matches with the Von Mises yield relation. The experimentally obtained universal value of $A = 1.73$ for yield correlation clearly shows that the deformation in shear punch test is shear dominant in the early stages of deformation. This enables direct estimation of tensile yield strength of irradiated alloys using shear punch tests using the 0.2% offset definition without requiring any other material specific constants.

3.3.2. Maximum strength correlation

The UTS and corresponding shear maximum strength (τ_{max}) of various alloys is plotted in Fig. 12. The linear correlation through origin yields a slope of 1.29 with $R^2 = 0.96$ and standard deviation of ±45 MPa. In the earlier work by Hamilton et al. [10], Hankin et al. [11] on various alloy systems, correlation equations of type $UTS = A_1\tau_{max} + B_1$ were established with slope (A_1) ranging from 1.8 to 2.9 and intercept B_1 ranging from −38 to −425 for various alloy classes. Similar linear correlations for tensile–shear maximum strength obtained in our earlier works using different heat treated and cold worked microstructural conditions of 2.25Cr–1Mo [5], Mod 9Cr–1Mo [12] and SS316 is reproduced in Fig. 13. The limited strength range over which the data were obtained for each alloy class could not force a best linear fit through origin and hence resulted in an intercept parameter B_1. Hamilton et al. suggested that the differences in the fit parameters between various alloys could be partly due to the size of the data base for each alloy class and partly due to punch–specimen–die friction. Based on these observations, a single correlation equation with a slope (A_1) of 2.2 for all alloy data sets [10] were arrived by Hamilton et al. only after subtracting the intercept values B_1 from the respective data sets.

Table 2
Tensile and shear punch test results of various materials studied.

Material	Tensile properties		Shear punch test properties			
	0.2% YS, MPa	UTS, MPa	Shear yield strength, MPa			Shear maximum strength, MPa
			0.2% offset	0.5% offset	1.0% offset	
Cu	127.14	202.00	56.74	64.71	74.02	158.00
Al	172.53	267.40	99.07	139.24	149.80	189.50
0.25% C steel	290.50	432.87	164.41	178.84	198.07	348.97
2.25Cr–1Mo	431.62	574.57	261.35	281.75	303.98	416.17
Mod 9Cr–1Mo	514.00	671.32	289.92	325.10	357.20	472.92
SS316	211.10	583.07	125.18	155.96	185.73	511.00

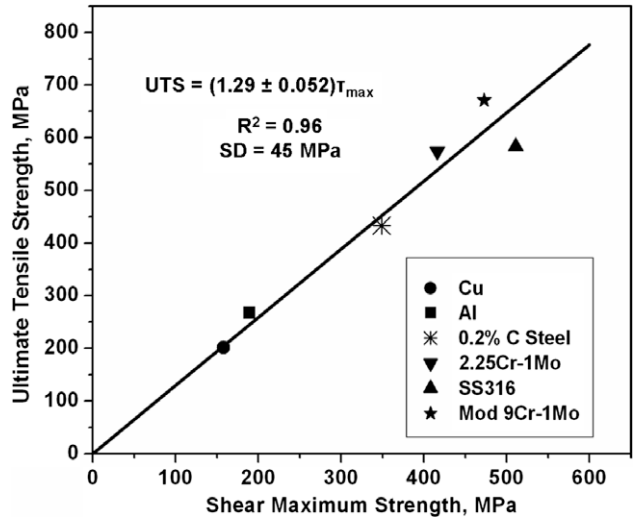

Fig. 12. The linear fit between UTS and shear maximum strength.

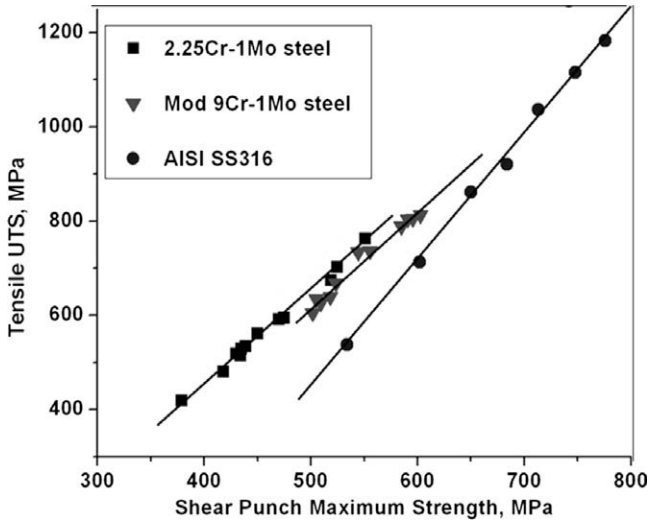

Fig. 13. UTS–shear maximum strength correlation of type UTS = $A\tau_{max} + B$ obtained for various alloys in authors laboratory [5,12].

However, to use this constant A_1 for predicting UTS from ShP data requires a prior knowledge of the B_1 parameter for the alloy.

It is seen that any attempt to predict UTS from shear punch test using a universal correlation of type UTS = $m\tau_{max}$ (m-constant) seems to be unreliable due to relatively poor R^2 and high standard deviation as compared to that of yield correlation. These observations suggest that the actual relation between the UTS and τ_{max} could be more complex involving some geometrical measure of deformation present in the shearing zone.

Ramaekars and Kals [13] studied the Von Mises equivalent strain of the blanked specimen from microhardness measurements on the specimen at various penetrations. The empirical relationship relating τ_{max} to UTS was derived as

$$\tau_{max} = s_f \mathrm{UTS}, \tag{4}$$

where s_f is the shearing factor equal to $\sqrt{\left\{\frac{1}{3}\left(\frac{3}{n}\right)^n\right\}}$,

n is the strain hardening exponent.

To verify the applicability of the above equation to our experimental data, τ_{max} estimated using Eq. (4) from known values of n from $\log\sigma - \log\varepsilon$ traces of tensile data and UTS is compared with

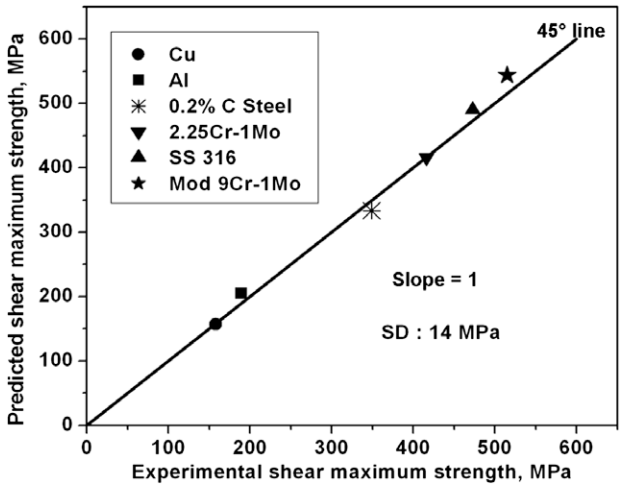

Fig. 14. Plot showing the excellent agreement between the experimental shear maximum strength and that predicted using Eq. (4).

the experimentally obtained τ_{max} and plotted in Fig. 14. A standard deviation of ±14 MPa indicates a good agreement between the experimental and predicted τ_{max}. The Eq. (4) relating the tensile and shear maximum strengths through strain hardening exponent 'n' is also found to be obeyed for all earlier data sets of 2.25Cr–1Mo, 9Cr–1Mo and SS316 generated in authors' laboratory.

The maximum strength correlation can thus be expressed as UTS = $m\tau_{max}$, where the coefficient $m = (1/s_f)$. Depending on 'n' value say 0.01–0.6, 'm' ranges from 1.68–1.06, indicating that the coefficient of the UTS correlation is always less than that of YS correlation. For a brittle material whose n is low, the coefficient m is close to 1.73 (same as yield correlation constant), while for a ductile material the 'm' reduces to around 1.10. Thus the lower values of UTS correlation coefficient 'm' as compared to yield correlation constant could be associated with the strain hardening capability of the material. For the materials investigated in the present study, the correlation coefficient 'm' averages to around 1.29 (Fig. 12). The Eq. (4) can also be used for predicting the 'n' value using UTS estimated through correlation of type UTS = $A_1\tau_{max} + B_1$ with known values of A and B. The following section analyses the evaluation of a strain hardening or ductility parameter from load–displacement data of ShP test.

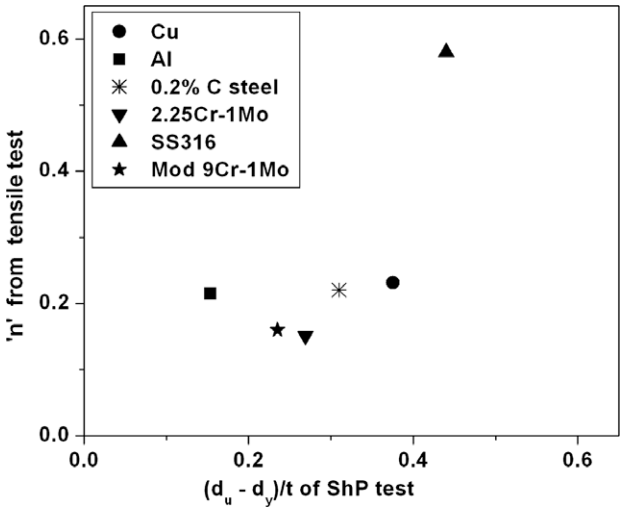

Fig. 15. Plot of 'n' from tensile test with the parameter $(d_u - d_y)/t$ of ShP test.

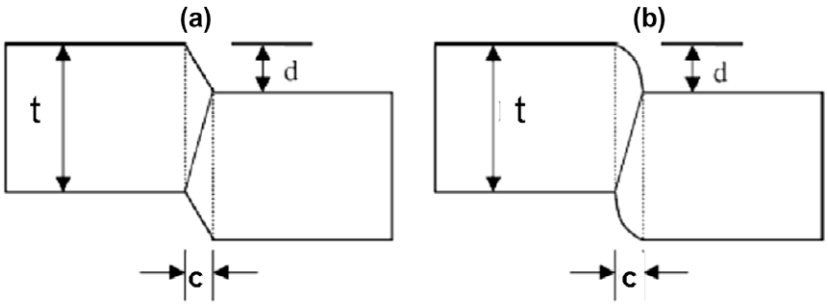

Fig. 16. Schematic of the shear deformation (a) pure shear and (b) with bending of the blank material fibers [16].

3.4. Strain hardening from shear punch test

One of the earlier approaches was to relate true strain in tensile tests to n_τ obtained from ShP data using the semi-empirical expression:

$$\left(\frac{n_\tau}{0.002}\right)^{n_\tau} = \left(\frac{\tau_{max}}{\tau_{ys}}\right), \tag{5}$$

where n_τ is the strain hardening exponent in ShP test [2]. The other approach is based on relating the true plastic strain or strain hardening exponent obtained in tensile test to the normalized displacement in ShP test. Fig. 15 shows the plot of strain hardening exponent 'n' from tensile data with $(d_u - d_y)/t$, where d_u/t and d_y/t are the normalized displacements at shear maximum strength and shear yield strength respectively. No distinct trend line is possible through the data sets indicating that a direct universal correlation of type $n = B(d/t)$, (B-constant) may not be possible.

An attempt was made to use the analytical model of Atkins [14] to analyze the LDC for strain hardening parameter. For the simple geometry of punching shown in Fig. 16a, assuming a power law behavior $\sigma = K\varepsilon^n$, where K is the strength coefficient and n is the strain hardening exponent, Atkins derived the punching force F with friction modeled through an assumed proportion f of the shear stress τ as

$$F = \pi D[(t-d) + 2f \cdot d]C_2\left(\frac{d}{c}\right)^n, \tag{6}$$

where D: diameter of the punch; d: punch penetration; c: width of the clearance zone; t: specimen thickness; C_2: constant in the power law $\tau = C_2\gamma^n$; γ: shear strain.

Using the Von Mises' expressions for equivalent stress and strain for assumed pure shear condition:

$$\tau = \frac{\sigma}{\sqrt{3}}, \tag{7}$$

$$\gamma = \sqrt{3}\varepsilon, \tag{8}$$

the constants C_2 and K are related through the expression $C_2 = K/(\sqrt{3})^{n+1}$.

This coupled with Ramaekars equation $\tau_{max} = \text{UTS}\ s_f$, where $\text{UTS} = K(n/e)^n$, $e = 2.71$, is used to derive an equation for d_u (displacement at peak load) in terms on 'n' and other parameters (assuming $f = 0$) as

$$(t-d_u)(d_u)^n = t(1.1c)^n(n)^{n/2}. \tag{9}$$

An estimate of n (n_{est}) obtained by solving the above equation with experimental values of d_u is compared with the strain hardening exponent 'n' from $\log\sigma - \log\varepsilon$ traces of tensile data as shown in Fig. 17. A good match is seen for low carbon steel, Mod 9Cr–1Mo and copper, while n_{est} is grossly underestimated for SS316. It may be noted that this model is based on assumptions of pure shear. Klingenberg et al. [15,16] modified the analytical model of Atkins to include bending (Fig. 16b) and frictional component during the blanking process for estimating the Von Mises equivalent stress and strain from force–displacement data. Analysis of the modified model with our ShP data reveals a trend almost similar to Fig. 17, with good match for estimated 'n' with tensile 'n' for low carbon steel, modified 9Cr–1Mo and copper alloys, while large differences are observed for austenitic steels. The assumptions of shear dominant deformation in punching with the simplified geometry of Fig. 16 and power law type of work hardening behavior needs further investigation for evolving an accurate analytical model for equivalent stress–strain values. The optimization of these analytical models together with finite element modeling of the non-linear deformation up to peak load form the basis for further research work in authors' laboratory.

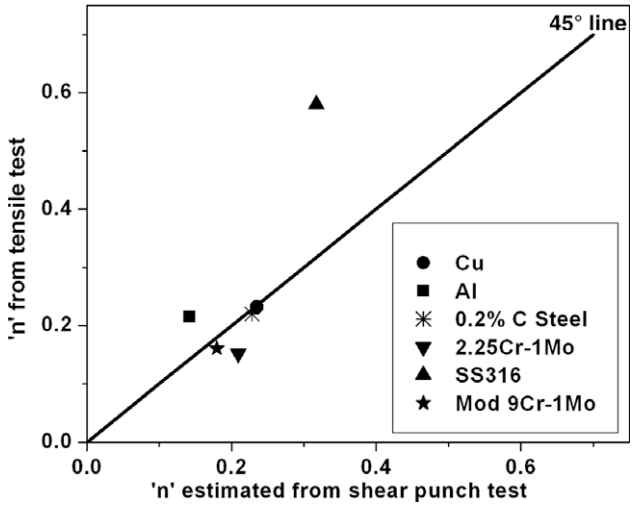

Fig. 17. Plot of 'n' estimated from shear punch test data using Eq. (9) compared with 'n' determined from tensile test.

4. Conclusions

A modified shear punch experimental setup in which specimen displacement is measured directly using an LVDT has been demonstrated to eliminate the effects of punch and die compliances on the load–displacement curve.

The shear yield strength evaluated using the 0.2% offset definition produces the best fit with the tensile yield strength and satisfies the Von Mises yield relation $\sigma_{ys} = 1.73\tau_{ys}$. The 0.2% offset definition for shear yield strength proposed in our experimental study is much less than 1% offset reported by earlier researchers due to the elimination of compliances of the fixture components. The offset definition is in close agreement with the 0.15% offset criterion obtained in finite element simulation studies by other investigators.

A universal correlation of type UTS = $m\tau_{max}$, where 'm' is a function of strain hardening exponent, is found to be valid for all alloys in this study. The value of coefficient 'm' is found to be always less than the yield correlation constant.

Analytical models of shearing process are found to be useful but with limited success for accurately predicting the strain hardening exponent from the load–displacement data. There is a need for modeling the non-linear deformation well beyond yielding in shear punch tests towards developing methodologies for accurate evaluation of the strain hardening parameter directly from the load–displacement data.

Acknowledgement

The authors gratefully acknowledge the encouragement and constant support of Dr. P.R. Vasudeva Rao, Director of Metallurgy and Materials Group, Indira Gandhi Centre for Atomic Research (IGCAR) during the course of the work.

References

[1] G.E. Lucas, J. Nucl. Mater. 117 (1983) 327.
[2] G.E. Lucas, G.R. Odette, J.W. Sheckherd, in: W.R. Corwin, G.E. Lucas (Eds.), The Use of Small-Scale Specimens for Testing Irradiated Materials, ASTM STP 888, 1988, p. 112.
[3] V. Karthik, K.V. Kasiviswanathan, K. Laha, Baldev Raj, Weld. J. (Res. Suppl.), AWS (2002) 265s.
[4] M.B. Toloczko, Y. Yokokura, K. Abe, M.L. Hamilton, F.A. Garner, R.J. Kurtz, in: M.A. Sokolov, J.D. Landes, G.E. Lucas (Eds.), Small Specimen Test Techniques, vol. 4, ASTM STP 1418, 2002, p. 371.
[5] V. Karthik, K. Laha, K.V. Kasiviswanathan, Baldev Raj, in: M.A. Sokolov, J.D. Landes, G.E. Lucas (Eds.), Small Specimen Test Techniques, vol. 4, ASTM STP 1418, 2002, p. 380.
[6] M.B. Toloczko, R.J. Kurtz, A. Hasegawa, K. Abe, J. Nucl. Mater. 307–311 (2002) 1619.
[7] R.K. Guduru, K.A. Darling, R. Kishore, R.O. Scattergood, C.C. Koch, K.L. Murty, Mater. Sci. Eng. A 395 (2005) 307.
[8] K.V. Kasiviswanathan, S.K. Hotta, C.K. Mukhopadhyay, Baldev Raj, in: W.R. Corwin, S.T. Rosinski, Evan Walle (Eds.), Small Specimen Test Techniques, ASTM STP 1329, 1998, p. 523.
[9] R.K. Guduru, A.V. Nagasekhar, R.O. Scattergood, C.C. Koch, K.L. Murty, Metall. Trans. 37A (2006) 1477.
[10] M.L. Hamilton, M.B. Toloczko, G.E. Lucas, Miniaturized specimens for testing of irradiated materials, in: Hans Ullmaier, Peter Jung (Eds.), IEA International Symposium, 1995, p. 46.
[11] G.L. Hankin, M.B. Toloczko, M.L. Hamilton, R.G. Faulkner, J.Nucl. Mater. 258–263 (1998) 1657.
[12] V. Karthik, K. Laha, P. Parameswaran, K.V. Kasiviswanathan, Baldev Raj, J. Test. Eval. 35 (2007) 438.
[13] J.A.H. Ramaekars, J.A.G. Kals, in: Proceedings of the IMC Conference, 1986, p. 126.
[14] A.G. Atkins, Int. J. Mech. Sci. 22 (1980) 215.
[15] W. Klingenberg, U.P. Singh, J. Mater. Process. Technol. 134 (2003) 296.
[16] W. Klingenberg, U.P. Singh, Int. J. Mach. Tool Manu. 45 (2005) 519.